Principles of Resonance Energy Transfer

Ágnes Szabó,[1,2] János Szöllősi,[1,2,3] and Peter Nagy[1,2]

[1]Department of Biophysics and Cell Biology, Faculty of Medicine, University of Debrecen, Debrecen, Hungary
[2]ELKH-DE Cell Biology and Signaling Research Group, Faculty of Medicine, University of Debrecen, Debrecen, Hungary
[3]Corresponding author: *szollo@med.unideb.hu*

Published in the Cytometry section

This unit describes the basic principles of Förster resonance energy transfer (FRET). Beginning with a brief summary of the history of FRET applications, the theory of FRET is introduced in detail using figures to explain all the important parameters of the FRET process. After listing various approaches for measuring FRET efficiency, several pieces of advice are given on choosing the appropriate instrumentation. The unit concludes with a discussion of the limitations of FRET measurements followed by a few examples of the latest FRET applications, including new developments such as spectral flow cytometric FRET, single-molecule FRET, and combinations of FRET with super-resolution or lifetime imaging microscopy and with molecular dynamics simulations. © 2022 The Authors. Current Protocols published by Wiley Periodicals LLC.

This article was corrected on 20 December 2022. See the end of the full text for details.

Keywords: flow cytometric FRET • fluorescence lifetime • Förster distance • Förster resonance energy transfer (FRET) • orientation factor • single molecule FRET

How to cite this article:
Szabó, Á., Szöllősi, J., & Nagy, P. (2022). Principles of resonance energy transfer. *Current Protocols*, *2,* e625. doi: 10.1002/cpz1.625

INTRODUCTION

Understanding the structural features of individual molecules or molecular complexes is the primary aim of cellular and molecular biological research. This knowledge provides detailed insight into biological responses and identifies druggable targets. Fluorescence-based approaches occupy an important place in such investigations due to their ease of application, biocompatibility, and the availability of many fluorescence kits. Even before the advent of superresolution techniques, a phenomenon based on the dipole-dipole interaction between atoms or molecules provided an opportunity to read out molecular details even in complex biological systems. This phenomenon is the Förster resonance energy transfer (FRET), which is almost exclusively measured by fluorescence techniques. However, the interaction itself has nothing to do with fluorescence, and the term fluorescence resonance energy transfer, often used as a synonym for Förster resonance energy transfer, is a misnomer. Unlike superresolution microscopy, FRET provides details about molecular interactions and requires much less sophisticated instrumentation. However, researchers applying it must be conversant with its principles and potential pitfalls to harness its full power and avoid misinterpreting experimental data. This unit is aimed at interested researchers planning to apply FRET in their research and will guide them through the principles and applications of the process along with its limitations.

CURRENT PROTOCOLS
A Wiley Brand

Current Protocols e625, Volume 2
Published in Wiley Online Library (wileyonlinelibrary.com).
doi: 10.1002/cpz1.625

HISTORY OF FRET

Interest in the quantitative interpretation of fluorescence began in the 20th century, coinciding with the great quantum physical revolution (Clegg, 2009). It was the Perrins, father and son, who, in the 1920s and 1930s, observed resonance energy transfer between fluorophores in solution. However, they failed to provide an accurate theoretical description of the process (Perrin, 1929, 1932). After Theodor Förster published his first account of nonradiative energy transfer assuming resonance between the significantly broadened electronic energy levels of fluorophores (Förster, 1946), it took several decades before FRET saw widespread application in biology. In the 1960s, Stryer and Haugland verified the theory and demonstrated that FRET measurements could be carried out with fluorescently labeled peptides (Stryer & Haugland, 1967). While FRET was initially applied in cuvette-based systems for ensemble measurements, technological advances have armed it with single-cell and subcellular resolution. Single-molecule FRET measurements even make it possible to discriminate one molecule from another based on conformation. The widespread availability of digital imaging microscopes and flow cytometers, as well as computers with enough power and the development of technologies based on monoclonal antibodies and fluorescent proteins, ushered in a new age in which FRET has become part of the armamentarium of cell and molecular biologists.

THEORY OF FRET

FRET is a physical process in which two molecules or atoms interact. The donor must be in the excited state and transfers energy to a nearby acceptor via intermolecular long-range, dipole-dipole coupling. This interaction is principally different from radiative energy transfer, in which photon emission and reabsorption mediate energy transfer. This trivial energy transfer process takes place with negligible probability at low ($<\mu$M) concentrations of fluorescent probes. In order for FRET to take place, several conditions must be met (Szabó, Szendi-Szatmári, Szöllősi, & Nagy, 2020):

1. Since the acceptor must be in the electric field of the donor, their separation distance has to be 2 nm to 10 nm (Stryer, 1978). If their distance is larger than 10 nm, the probability of FRET is negligibly small. Electron exchange interactions occur if the interacting molecules are less than 2 nm from each other (Marcus, 1993). The distance range of 2 nm to 10 nm corresponds to macromolecular dimensions and intermolecular interactions, which form the basis of the application of FRET in biological research. Within this distance range, the probability of FRET decays steeply with increasing separation between the donor and the acceptor, a feature that is going to be discussed later in more detail.
2. The donor and acceptor must be properly oriented relative to each other. It is a common misconception that the angle between the donor and acceptor determines the orientation dependence of FRET. An easy way to visualize this orientational requirement is to think of the donor and acceptor as radio antennas. The donor antenna generates an electric field, and the more parallel the acceptor antenna is to the electric field of the donor, the stronger their interaction will be. In other words, it is not the orientation of the donor and acceptor per se but the orientation of the acceptor relative to the electric field of the donor that matters most (Van der Meer, 2020). While the sensitivity of FRET to orientation can be harnessed in biological applications, it is most often a source of problems since it confounds the relationship between the probability of FRET and distance, the property most biologists are interested in. Therefore, this condition will be more closely considered in a subsequent section.
3. The energy released by a relaxing donor must equal the energy required by the acceptor to get excited. This condition is met if the donor emission spectrum and the acceptor absorption spectrum overlap (Fig. 1). In conventional FRET, the donor and acceptor are different kinds of molecules having sufficient spectral overlap. This kind of interaction is termed hetero-FRET and is usually what is meant when FRET is mentioned without attribute. Since the absorption and emission spectra of most fluorophores overlap, this spectral condition can also be met by two identical fluorophores in an interaction termed homo-FRET. While the principle of this process is identical to that of hetero-FRET, its measurement is difficult because homo-FRET only alters the fluorescence anisotropy, a limitation that will be discussed further in subsequent sections. The extent of overlap is characterized by the overlap integral (J) according to the following equation:

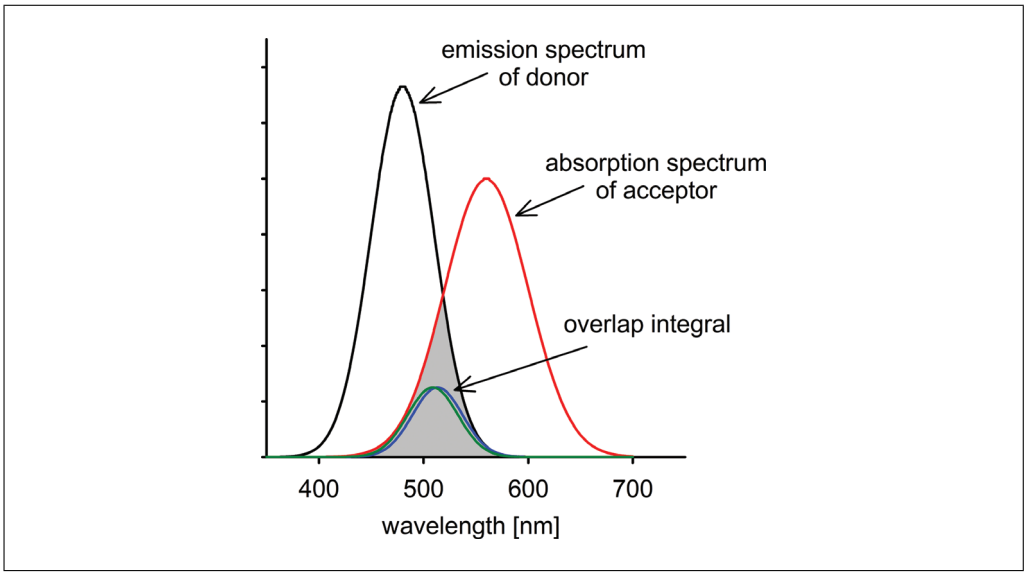

Figure 1 The overlap integral. The donor emission and acceptor absorption spectra are shown in black and red, respectively. The spectra must overlap for FRET to take place, a condition that corresponds to the "resonance" between donor and acceptor. The overlap is usually represented by the gray shaded area. However, the overlap integral is not simply the graphical overlap between the two spectra, and due to its dependence on the fourth power of the wavelength (equation (1)), high wavelengths are slightly overweighted. The blue curve shows the overlap integral correctly calculated according to equation (1), while the green curve shows the incorrect overlap integral determined without the λ^4 term. Comparison of the blue and green curves reveals that long wavelengths are given slightly more weight.

$$J = \int F_D(\lambda)\,\varepsilon_A(\lambda)\,\lambda^4 d\lambda$$

Equation 1

where $F_D(\lambda)$ is the corrected, wavelength-dependent fluorescence intensity of the donor with the total intensity (area under the curve) normalized to unity, and $\varepsilon_A(\lambda)$ is the molar absorption coefficient of the acceptor.

If the conditions above are satisfied, resonance interaction between donor and acceptor takes place:

$$D^* + A \underset{k-T}{\overset{k_T}{\rightleftarrows}} D + A^*$$

Equation 2

where D and A denote the donor and acceptor in the ground state, D^* and A^* denote their excited states, and k_T and k_{-T} denote the rate constants of the forward and reverse transfer processes, respectively. To ensure FRET is a unidirectional process, the rate constant of the forward reaction must be significantly larger than the rate constant of the reverse process. However, if there is resonance between the donor and acceptor, one may ask why the forward and reverse processes are not equally likely. Fast, non-radiative transitions lead to the relaxation of the acceptor before back-transfer can occur. Therefore, the acceptor is no longer in resonance with the donor, and back-transfer becomes practically impossible (Fig. 2). According to Förster's theory, the rate constant of FRET, k_T, is given by the following equation:

$$k_T = const k_F J n^{-4} R^{-6} \kappa^2$$

Equation 3

where k_F is the rate constant of fluorescence of the donor, J is the overlap integral specified by equation (1), n is the index of refraction of the medium between the donor and acceptor, κ^2 is the orientation factor (see later in equation (9)), and R is the distance between the donor and acceptor. This equation reveals several fundamental and practically important features of FRET:

– Its rate constant decays with the sixth power of the separation distance between donor and acceptor, making FRET a sensitive tool to measure molecular distances and oligomerization (Fig. 3).

- It is proportional to the rate constant of fluorescence of the donor. Consequently, the more fluorescent the donor is, the more likely FRET will be. For this reason, the fluorescence quantum efficiency of the donor must be considered when choosing a suitable donor for FRET measurements.

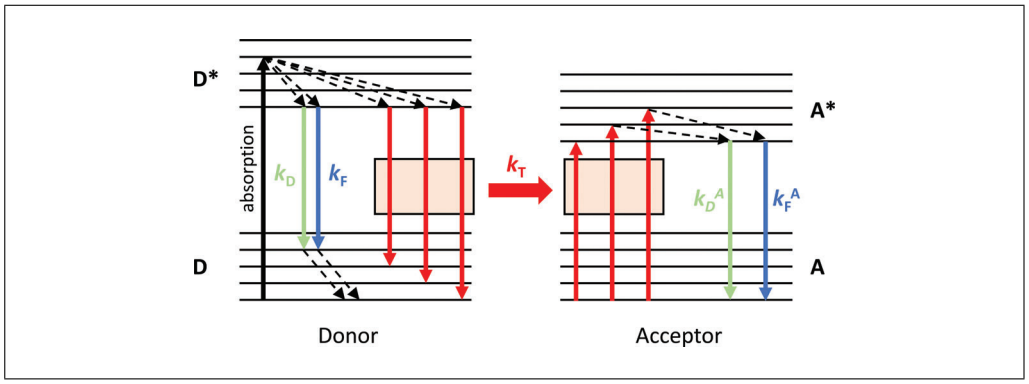

Figure 2 The energy balance of the FRET interaction. The donor is excited from its ground state (*D*) to its excited state (*D**), typically followed by nonradiative relaxation (oblique dashed lines) to the lowest subshell of the first excited state in an extremely short time (in less than 1 ps). In the absence of an acceptor, the donor can return to the ground state via non-radiative transitions and fluorescence characterized by the rate constants k_D and k_F, respectively. If a suitable acceptor is present in the immediate vicinity of the donor, relaxation of the donor can be coupled to excitation of the acceptor via FRET (red arrows). While several donor de-excitation transitions can be coupled to acceptor excitation transitions, these can only take place if the energy released during donor relaxation is equal to the energy required for acceptor excitation. This is a manifestation of the resonance condition and is shown in the figure by the same lengths of the downward and upward red arrows. The FRET rate constant, k_T, characterizes all the possible dipole-dipole couplings between the donor and the acceptor. After energy transfer, the excited acceptor relaxes to the lowest subshell of its excited state in less than 1 ps (oblique dashed lines) just as the donor did. This rapid energy loss eliminates the resonance condition, making back-transfer impossible. Afterwards, the acceptor relaxes to the ground state by non-radiative or radiative transitions characterized by rate constants $k_D{}^A$ and $k_F{}^A$, respectively.

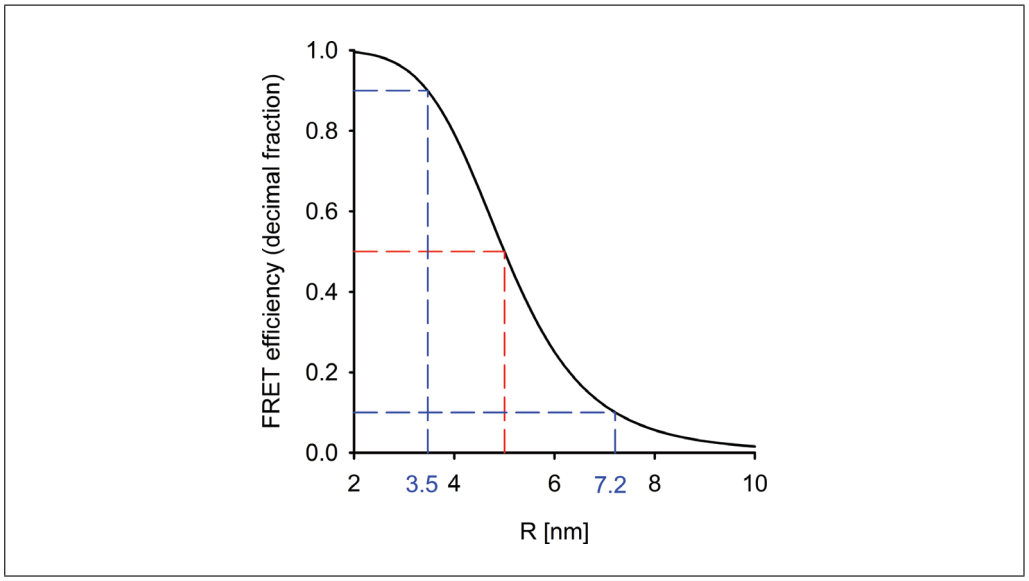

Figure 3 Dependence of FRET efficiency on donor-acceptor separation distance. FRET efficiency declines as a function of donor-acceptor distance (*R*) according to equation (6) in a single donor-acceptor pair characterized by a Förster distance of $R_0 = 5$ nm. FRET efficiency steeply declines around R_0, and declines from 0.9 to 0.1 in the distance range between $R = 0.7\ R_0$ and $R = 1.45\ R_0$ corresponding to 3.5–7.2 nm for an R_0 of 5 nm. Outside this distance range there is almost no change in FRET efficiency. Red lines show R_0, and blue lines correspond to the distance range in which the FRET efficiency declines from 0.9 to 0.1.

- The relative orientation of the donor and acceptor, expressed by the term κ^2, and the overlap integral (J) are proportional to the FRET rate constant. Therefore, the overlap integral must be considered when choosing a suitable donor-acceptor pair. More consideration will be given to the orientation factor in a subsequent section.
- The refraction index is usually 1.4 in biological measurements in aqueous solutions (Lakowicz, 2006a). However, it has been pointed out that the refraction index of the medium between the donor and acceptor can significantly deviate from this value, leading to errors in the calculations (Knox & van Amerongen, 2002). The uncertainty in the value of the refractive index is a problem only if absolute distances are to be determined. When relative changes in the FRET efficiency are calculated, the uncertainty in the index of refraction is not an issue since it is unlikely to change significantly.

While the previous equation describes the fundamental principles of FRET, it has usually been deemed too complicated for experimental determination. However, a recent publication noted subtle advantages of determining k_T compared to the energy transfer efficiency usually calculated (Roberti, Giordano, Jovin, & Jares-Erijman, 2011).

The energy transfer efficiency, E, is an easily understood parameter equal to the fraction of excited donors relaxing by FRET:

$$E = \frac{\text{number of quanta transferred from donor to acceptor}}{\text{number of quanta absorbed by the donor}}$$

Equation 4

According to Figure 2, excited donors return nonradiatively to the lowest energy level of the first excited state, and all further relaxation processes begin from this level. Consequently, these de-excitation processes compete with each other and can be expressed by the following equation, which presents another interpretation of energy transfer efficiency:

$$E = \frac{k_T}{k_T + k_F + k_D}$$

Equation 5

where k_T is the rate constant of FRET (equation (3)), k_F and k_D are the rate constants of fluorescence and all other relaxation processes of the donor, respectively. Neither of the previous two expressions for the FRET efficiency explicitly shows its distance dependence, a shortcoming that is remedied by the following equation:

$$E = \frac{{R_0}^6}{{R_0}^6 + R^6}$$

Equation 6

where R is the donor-acceptor distance and R_0 is a constant for a particular donor-acceptor pair giving that donor-acceptor separation at which the energy transfer efficiency is 50%. While the previous equations present three different ways to calculate FRET efficiency, none is usually used for its determination since the parameters in these equations are inaccessible to experimental determination. In "Measurement modalities for FRET" we discuss how energy transfer efficiency can be determined in practice.

The previous considerations did not cover a scenario in which multiple acceptors surround a single donor. In particular, equations (5) and (6) apply to a one donor-one acceptor case. If multiple acceptors surround a single donor the transfer rate and energy transfer efficiency are described by the following equations:

$$E = \frac{Nk_T}{Nk_T + k_F + k_D}$$

Equation 7

$$E = \frac{N{R_0}^6}{N{R_0}^6 + R^6}$$

Equation 8

where N is the number of acceptors surrounding the donor (Lakowicz, 2006b). For these equations to hold, all acceptors must be at the same distance from the donor, and all of them have to be in the ground state when the donor is excited so that they are ready to accept the energy transfer. This latter requirement is fulfilled at conventional excitation intensities. These equations reveal that more acceptors lead to a higher energy transfer efficiency even without a change in R. This principle is important for interpreting experimental FRET efficiencies and changes thereof. An increased energy transfer efficiency can result from a closer spacing of the donor and acceptor (decreased R), or it can be due to an increase in N, i.e., enhanced clustering.

Averaging Schemes of the Orientation Factor

As noted above, the FRET efficiency depends on the distance between donor and acceptor and their relative orientation. From an

experimental point of view, the relative orientation of donor and acceptor is difficult to measure, and in most cases, it can only be estimated from anisotropy measurements (Dale & Eisinger, 1974; van der Meer, van der Meer, & Vogel, 2013). Except for some structural biological problems, the dependence of FRET on orientation is a shortcoming since researchers are usually interested in the distance between donor and acceptor, not their orientation. The following equation gives two different expressions for the orientation factor, κ^2, at a fixed donor-acceptor configuration (Fig. 4):

$$\kappa^2 = (\cos\theta_T - 3\cos\theta_D \cos\theta_A)^2$$
$$= \cos^2\omega\left(1 + 3\cos^2\theta_D\right)$$

Equation 9

where θ_T is the angle between the donor emission dipole and the acceptor absorption dipole, θ_D is the angle between the donor emission dipole and the vector connecting the donor and the acceptor, θ_A is the angle between the acceptor absorption dipole and the vector connecting the donor and the acceptor, and ω is the angle between the absorption dipole of the acceptor and the electric field generated by the donor. It is obvious from the second part of the equation that $\kappa^2 = 0$ if the acceptor absorption dipole is perpendicular to the electric field generated by the donor (if $\omega = 90°$, $\cos\omega = 0$). This equation is of little practical value because these angles are unknown and experimentally difficult to estimate when biomolecules are labeled with fluorescent proteins or an organic fluorophore. To make things even worse, the orientation of the acceptor relative to the donor is not constant but different for distinct donor-acceptor pairs in a system. It may change during the excited state lifetime of the donor, a complication that actually comes to our relief.

If both the donor and acceptor are mobile to the extent that they rotate rapidly on the time scale corresponding to the excited state lifetime of the donor (typically a couple of nanoseconds), dynamic averaging takes place. In this case, the relative orientation of the donor and acceptor takes on all possible values during a single excitation of the donor. Instead of calculating the probability of FRET considering every possible relative orientation of the donor and the acceptor, κ^2 can be replaced by an average value, which was determined to be 2/3. Strictly speaking, this is the case, and the only case when equation (6) holds, i.e. FRET depends only on the donor-acceptor distance and not on their relative orientation if dynamic averaging takes place. To make the subsequent discussion more straightforward, let us rewrite equation (6) according to van der Meer (2002):

$$\langle E_{dynamic}\rangle = \frac{3/2\langle\kappa^2\rangle R_0^6}{3/2\langle\kappa^2\rangle R_0^6 + R^6}$$

Equation 10

where R_0 is the Förster distance when $\kappa^2 = 2/3$ and the brackets denote averages. Since, in the case of dynamic averaging $\kappa^2 = 2/3$, this equation reduces to equation (6). In every other case, the orientation of the donor and acceptor cannot be averaged independently, as in equation (10). Instead, the mean energy transfer efficiency must be calculated directly:

$$\langle E_{static}\rangle = \left\langle \frac{3/2\kappa^2 R_0^6}{3/2\kappa^2 R_0^6 + R^6} \right\rangle$$

Equation 11

According to this equation, the energy transfer efficiency has to be calculated for every relative orientation of the donor and acceptor, and the resulting FRET efficiencies are to be averaged. This approach presents a formidable task that can never be worked out practically in cell biological research. The question then becomes, how certain can we be that the approximation via dynamic averaging implicit in equation (6) is valid? If molecular distances are to be calculated, the potential mistakes can be relatively large if caution is not taken to prove dynamic averaging or to take κ^2 explicitly into consideration. On the other hand, when oligomerization or clustering of fluorescently labeled biomolecules is to be studied, most experimental results involving FRET assuming dynamic averaging of κ^2 are consistent with other results, arguing that the relative orientation of the donor and the acceptor are averaged enough so that the measured FRET efficiencies are primarily influenced by the donor-acceptor distance.

How to Choose a Donor-Acceptor Pair

Equation (6) includes the Förster distance, R_0, which is a guide for choosing an optimal donor-acceptor pair. It can be derived from other parameters according to the following equation:

$$R_0 = const\sqrt[6]{J\kappa^2 Q_D n^{-4}}$$

Equation 12

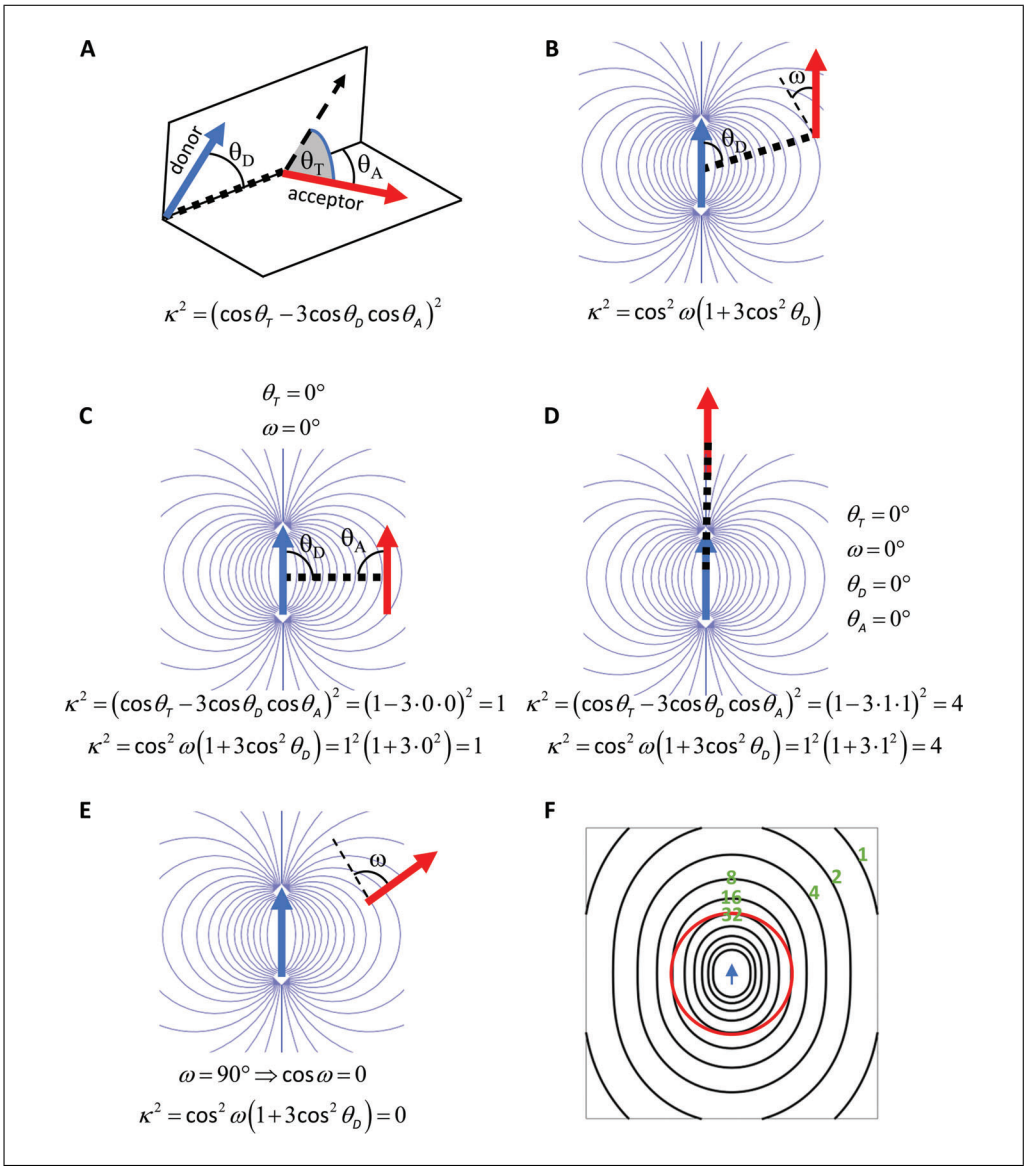

Figure 4 Interpretation of the κ^2 orientation factor. **(A)** Calculation of κ^2 according to equation (9). θ_T is the angle between the donor (blue vector) and acceptor (red vector) dipoles, θ_D is the angle between the donor emission dipole and the line connecting donor and acceptor (dashed line), whereas θ_A is the angle between the acceptor absorption dipole and the line connecting donor and acceptor. **(B)** Another calculation of the orientation factor. The definition of θ_D is the same as in part A, while ω is the angle between the acceptor absorption dipole and the electric field generated by the donor. The electric field lines are shown by the thin blue lines. **(C)** Calculation of κ^2 when the donor and acceptor dipoles are parallel and placed side-by-side. Since the two vectors are parallel, $\theta_T = 0°$, and since both dipoles are perpendicular to the line connecting donor and acceptor, $\theta_A = \theta_D = 90°$. Since the acceptor absorption dipole is parallel to the donor's electric field, $\omega = 0°$. Both formulas provide a value of 1 for κ^2. **(D)** All angles are zero and both formulas yield the highest possible value of 4 for κ^2. This is the only kind of arrangement of the donor and the acceptor when the orientation factor is the maximum. **(E)** When the acceptor absorption dipole is perpendicular to the electric field of the donor, the orientation factor is always zero. **(F)** Why is the orientation factor not identical in parts **C** and **D** although the donor and acceptor dipoles are parallel and equidistant in both cases? The black contour lines connect points having a magnitude equal to that of the electric field generated by a dipole (**Griffiths, 2013**). The blue vector in the middle shows the orientation of the dipole. Although the electric field of a dipole declines with the third power of the distance, its magnitude depends on the direction. The graph shows that the electric field extends farther in the direction parallel to the dipole. The red circle labels points equidistant from the dipole showing that the electric field is twice as strong at the point along

(legend continues on next page)

the dipole vector than it is at 90° to the dipole since the contour lines are logarithmically placed, and every consecutive contour level toward the center corresponds to a two-fold increase in the electric field (**Griffiths, 2013**). The green numbers show the electric field in arbitrary units for the outermost contours. Since the rate of FRET is proportional to the square of the donor's electric field (**van der Meer, 2013**), there will be a four-fold difference between the κ^2 values for the two positions (shown in **C** and **D**). The inverse sixth power dependence of the FRET rate on the donor-acceptor separation can be explained along the same lines. Although the donor's electric field falls off with the third power of the distance, the rate of FRET is proportional to the square of the donor's electric field, leading to the dependence of FRET on the sixth power of the donor-acceptor distance.

where Q_D is the fluorescence quantum yield of the donor in the absence of the acceptor. As a rule of thumb, the higher the Förster distance for a certain donor-acceptor pair, the better they are. Furthermore, the selected donor-acceptor pair should have a characteristic Förster distance of at least 5 nm. How can this aim be achieved according to the previous equation?

- The overlap integral (J) must be as high as possible. However, if the emission spectrum of the donor exhibits a very large overlap with the absorption spectrum of the acceptor, their spectral separation may not be large enough, potentially leading to significant spectral overspills between the detectors measuring donor and acceptor fluorescence.
- The fluorescence quantum yield of the donor in the absence of the acceptor must also be as high as possible. Measuring FRET using donors with very low fluorescence quantum efficiencies becomes practically impossible.
- In most biological applications of FRET in which the donor-acceptor distance or the clustering of donor- and acceptor-tagged molecules are to be determined, it is usually preferred to have the fluorophores linked to the molecules of interest via flexible linkers that allow dynamic averaging to take place. This scenario essentially eliminates the dependence of FRET on orientation. Due to their small size, organic fluorophores usually rotate rapidly on the nanosecond time scale approximating, but most likely not fully meeting the requirements of, dynamic averaging (Bene, Fulwyler, & Damjanovich, 2000; Bene et al., 2005). Fluorescent proteins should be connected via flexible peptide linkers to the molecule under investigation. Such peptide linkers behave as random coils and allow a large degree of flexibility for the fluorophore (Evers, van Dongen, Faesen, Meijer, & Merkx, 2006).
- FRET reports the distance between donor and acceptor fluorophores, although the investigator is usually interested in the distance between or clustering of the labeled molecules. Consequently, the size of the fluorophore confounds interpretation of the experimental results. Therefore, small fluorophores are preferred for labeling, not only because of this argument, but also to minimize the perturbing effect of the label on the target of interest. In particular, if the fluorophore is part of a large labeling complex, the labeling complex can hold the donor and acceptor apart, preventing FRET from taking place. If no FRET is observed in a certain experiment, this kind of artifact must be considered in the interpretation.

Since R_0 plays such a central role in selecting a suitable donor-acceptor pair, several tools have been developed for its calculation:

- The "FPbase FRET Calculator" determines R_0 for many organic dyes and fluorescent proteins (*https://www.fpbase.org/fret/*).
- The Förster distances of commonly used Alexa Fluor dye pairs are available on the manufacturer's website (*-https://www.thermofisher.com/hu/en/home/references/molecular-probes-the-handbook/tables/r0-values-for-some-alexa-fluor-dyes.html*).
- An Excel file and a MATLAB application are available for calculating the Förster distance on the web page of one of the authors
- (*https://peternagyweb.hu/FRET.html#r0_section*).

MEASUREMENT MODALITIES FOR FRET

Changes induced by the occurrence of FRET in measurable parameters can be deduced from the physical process itself. Every manifestation of FRET corresponds to a measurement approach (Jares-Erijman & Jovin, 2003):

- Energy transfer is an extra de-excitation process for the donor competing with fluorescence and other non-fluorescent relaxation pathways. Consequently, fluorescence is less likely to occur, resulting in donor

quenching, i.e., decreased donor fluorescence intensity. The FRET efficiency can be calculated from the fractional decrease in donor intensity:

$$E = 1 - \frac{I_{DA}}{I_D}$$

Equation 13

where I_{DA} and I_D are the donor intensities in the presence and absence of the acceptor, respectively. Rearrangement of this equation shows that the decrease in measured donor intensity is proportional to the FRET efficiency and intensity of the donor in the absence of FRET:

$$I_D - I_{DA} = EI_D$$

Equation 14

These formulas explain why FRET measurements are more reliable if donors with high fluorescence quantum yields are used. Equation (13) is rarely used for calculating the FRET efficiency because:

- The donor intensity is nearly always contaminated by directly excited or FRET-sensitized acceptor emission; therefore, spectral compensation is necessary.
- The equation involves two intensities measured in two different samples. I_{DA} is measured in a donor-acceptor double-labeled sample, whereas I_D is the intensity of the donor-only sample. To ensure equation (13) holds, the difference between I_{DA} and I_D has to be the sole consequence of FRET. Statistical variation in the expression level of the donor-labeled target between the donor-only and donor-acceptor double-labeled samples may result in differences in the unquenched donor intensity of these two samples; thus, the requirement formulated in the previous sentence is not met. This issue is especially important if measuring a small number of cells. If, however, the acceptor can be turned off in one way or another, both I_D and I_{DA} can be measured in the same sample. Such an achievement has been demonstrated by photodestruction of the acceptor (acceptor photobleaching) (Bastiaens, Majoul, Verveer, Soling, & Jovin, 1996), saturating the acceptor (Beutler et al., 2008), or by reversibly photoswitching the acceptor (Song, Jares-Erijman, & Jovin, 2002).

- Since the donor has more options for relaxation in the presence of FRET, it will spend less time in the excited state. Consequently, the fluorescence lifetime of the donor will decrease according to the following equation:

$$E = 1 - \frac{\tau_{DA}}{\tau_D}$$

Equation 15

where τ_{DA} and τ_D are the fluorescence lifetimes of the donor in the presence and absence of the acceptor, respectively. Measurement of the decreased donor fluorescence lifetime requires either time-domain or frequency-domain lifetime measurements (Becker, 2012).

- The fact that the donor spends less time in the excited state makes any excited-state reaction of the donor slower. Donor photobleaching is such a reaction, which becomes consequently slower (Bastiaens et al., 1996):

$$E = 1 - \frac{\tau_{bl,\,D}}{\tau_{bl,\,DA}}$$

Equation 16

where $\tau_{bl,D}$ and $\tau_{bl,DA}$ are the photobleaching time constants of the donor in the absence and presence of the acceptor, respectively.

- Anisotropy is a measure of the polarized nature of fluorescence emission that can be measured after polarized excitation followed by polarized emission detection. If a fluorophore is excited by vertically polarized light, fluorescence anisotropy (r) is defined according to the following equation (Lakowicz, 2006c):

$$r = \frac{I_{VV} - I_{VH}}{I_{VV} + 2I_{VH}}$$

Equation 17

where I_{VV} and I_{VH} are the vertical and horizontal components of the fluorescence emission, respectively. The higher the intensity of the vertical component compared to the horizontal one, the higher anisotropy is. After vertical excitation, the fraction of horizontally polarized emission increases if the fluorophore rotates. If the donor has less time to rotate during its excited state due to a FRET-dependent shortened lifetime, I_{VH} will be smaller, leading to a higher anisotropy according to the following equation (Bene et al., 2000; Matkó, Jenei, Mátyus, Ameloot, & Damjanovich, 1993):

$$\frac{1}{r} = \frac{1}{r_0}\left(1 + \frac{\tau_D\,(1-E)}{\theta}\right)$$

Equation 18

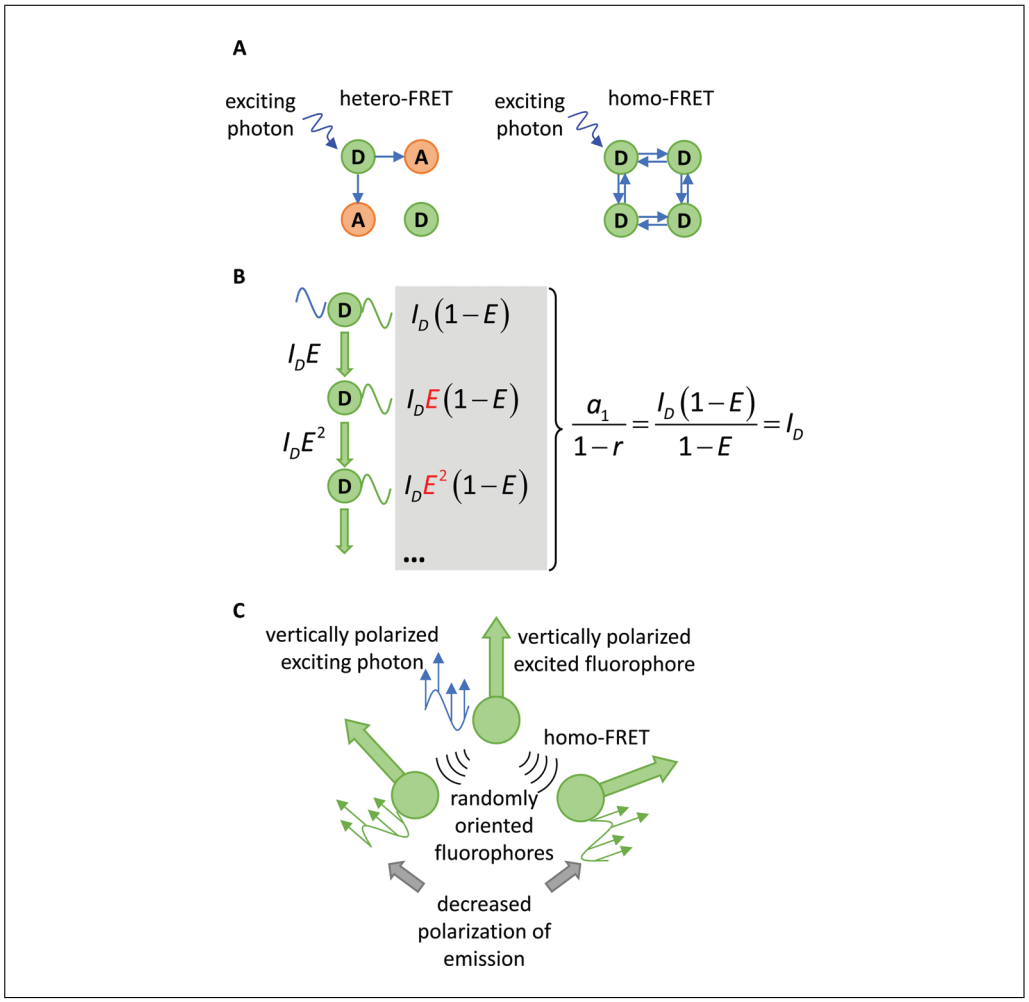

Figure 5 Principles of homo-FRET. **(A)** Hetero-FRET is a unidirectional process. Therefore, the energy imparted upon the donor will only spread to nearby acceptors, and not to the whole complex. Although statistical considerations can reveal the cluster size in hetero-FRET, homo-FRET is inherently sensitive to oligomerization. This phenomenon is due to the fact that the donors and acceptors are spectroscopically identical in homo-FRET and an acceptor can transfer the energy back to the original donor or pass it on to another nearby fluorophore. **(B)** Photons emitted by all fluorophores in a homo-FRET process are indistinguishable. The primarily excited fluorophore emits an intensity of $I_D(1-E)$, where I_D is its unquenched fluorescence intensity and E is the FRET efficiency. A fraction of the excitation intensity of this primarily excited donor (I_D E) is passed to a nearby acceptor, which is spectroscopically identical to the donor. This principle is repeated for every subsequent donor, i.e., a fraction of (1-E) of the energy of a donor is emitted, and a fraction of E is passed on to the next fluorophore. Although the primary donor is quenched, i.e., its intensity decreases from I_D to $I_D(1-E)$, this intensity decrease is unmeasurable since all the emitted photons are indistinguishable. The intensity is the sum of an infinite geometric series (gray box) that can be calculated according to the formula on the right, in which a_1 and r are the first term in the series, $I_D(1-E)$, and the common ratio, E, respectively. Substituting these values into the formula reveals that the intensity is identical to the unquenched intensity of the primarily excited donor, i.e., no intensity decrease takes place as a result of homo-FRET. **(C)** The only manifestation of homo-FRET is decreased fluorescence anisotropy. Excitation of a donor with vertically polarized light results in a photoselected population of excited donors exhibiting a preferential vertical orientation. The polarized nature of the emission (anisotropy) from this primarily excited donor is decreased by the rotation of the fluorophore during the excited state (not shown in the figure). Although FRET, including homo-FRET shows some preference for orientation expressed by the κ^2 orientation factor, the fluorophores secondarily excited by homo-FRET are relatively randomly oriented. Therefore, the anisotropy of the emission from a cluster in which energy is distributed by homo-FRET decreases.

where r_0 is the limiting anisotropy of an immobile fluorophore and θ is its rotational correlation time. Measurement of FRET efficiency according to this approach requires polarized excitation and polarized emission detection.

- As pointed out in the theory section, even if the donor and acceptor are fluorophores of the same kind, they can still interact with each other by FRET. Energy transfer in these cases is called homo-FRET. Although the principles of homo-FRET are identical to those of conventional, hetero-FRET, this flavor of resonance energy transfer has certain differences of practical importance. Since a single kind of fluorophore takes part in the process, the acceptor fluorophore can act as a donor, and therefore an infinite number of FRET steps can take place. In other words, the excitation energy is distributed among the population of fluorophores within FRET distance of each other. Based on this principle, it can be shown that no ensemble parameter of the fluorophore changes, other than its anisotropy (Fig. 5). However, why does the anisotropy change if there is no alteration in the lifetime? Although the FRET interaction does have a certain orientational preference expressed by κ^2, the population of fluorophores excited by homo-FRET is still more randomly oriented than the photoselected fluorophore population excited by the polarized excitation source. Since photons emitted by fluorophores primarily excited by the polarized light source and those emitted by fluorophores excited by homo-FRET are indistinguishable, the average anisotropy of the photons emitted by the ensemble of fluorophores decreases. It has been shown that the anisotropy decreases with the number of fluorophores within homo-FRET distance of each other (Runnels & Scarlata, 1995). Since anisotropy changes due to homo-FRET and rotational mobility, experimentally linking anisotropy and changes thereof to homo-FRET is challenging. Experimental models have been devised in which the dependence of anisotropy on the local density of fluorophores is utilized for determining the number of fluorophores within FRET distance of each other (Lidke et al., 2003; Szabó, Horváth, Szöllősi, & Nagy, 2008; Yeow & Clayton, 2007).
- Just as the evaluation of donor intensity in the presence and absence of FRET according to equation (13) presents a way to calculate energy transfer efficiency, a comparison of acceptor intensity in the presence and absence of a donor also makes FRET determination possible. In any realization of this principle, the donor-acceptor system is excited at the donor wavelength and fluorescence is recorded at the acceptor emission wavelength. Since in most practical cases the acceptor can also be excited at the donor wavelength (direct acceptor fluorescence), the extra acceptor fluorescence due to donor excitation and subsequent FRET to the acceptor (FRET-sensitized acceptor fluorescence) has to be separated:

$$\frac{F_{AD}}{F_A} = 1 + \frac{\varepsilon_D c_D}{\varepsilon_A c_A} E$$

Equation 19

where F_{AD} and F_{A} are the fluorescence intensities of the acceptor in the presence and absence of the donor, respectively, ε and c are the molar absorption coefficient and the molar concentration, respectively, and lower indices in these variables refer to the donor (D) and acceptor (A). F_{A} is the directly excited acceptor fluorescence at the donor excitation wavelength, whereas F_{AD} is the sum of directly excited and FRET-sensitized acceptor emissions. Equation (19) is of little practical value for cell biological FRET measurements for the very same reasons as explained in equation (13).

While discussing the technical details of such intensity-based FRET measurements is not the aim of the current chapter, the general principles of these approaches are similar. In order to compensate for spectral crosstalk and eliminate the need to compare intensities measured in different samples (such as in equations (13) and (19)), intensities are typically measured in three detection channels (Table 1).

None of these channels records pure intensities since spectral spillover is usually present. Therefore, the equation set must always include spectral spillover factors characterizing the overspill of intensities between different detection channels. Another parameter, variably termed α, G, or ω, is also required for intensity-based FRET measurements because donor intensity is lost in the donor channel due to donor quenching; thus, part of this intensity appears as acceptor fluorescence in the FRET channel. This calibration factor relates these intensities to each other (Szabó & Nagy, 2021). A detailed explanation of the equations involved in intensity-based FRET measurements is available in the

Table 1 Excitation and Detection Wavelengths for Intensity-Based FRET Measurements

	Excitation wavelength	Detection wavelength range
Donor channel	Donor excitation wavelength	Donor emission wavelengths
FRET channel		Acceptor emission wavelengths
Acceptor channel	Acceptor excitation wavelength	

"Measuring FRET in flow cytometry and microscopy" Current Protocols in Cytometry chapter (Nagy, Vereb, Damjanovich, Mátyus, & Szöllősi, 2006). A critical comparison of these methods has also been published (Zeug, Woehler, Neher, & Ponimaskin, 2012).

- Since either the donor or the acceptor emits, emission from a FRET sample is composed of two different spectral signatures. The acceptor emission can be the consequence of direct or FRET-sensitized acceptor excitation. Using the spectral signature of a known concentration of donor and acceptor and measuring the spectrum of a FRET sample containing donors and acceptors at two different excitation wavelengths, it is possible to derive the concentrations of the donor and acceptor and the FRET efficiency (Thaler, Koushik, Blank, & Vogel, 2005). Such measurements can be carried out in fluorimeters, spectral confocal microscopes that have become widespread, leading to a proliferation of publications applying spectral FRET analysis (Chen, Mauldin, Day, & Periasamy, 2007; Leavesley, Britain, Cichon, Nikolaev, & Rich, 2013; Wlodarczyk et al., 2007; Zeug et al., 2012). Such measurements can be carried out in spectral flow cytometers (Henderson et al., 2021) and in fluorimeters, spectral confocal microscopes.
- Acceptor fluorescence is increased by FRET because energy transfer results in an enhanced population of excited acceptors. This principle can be extended to any reaction starting from the excited state of the acceptor, such as acceptor photobleaching. FRET-sensitized acceptor photobleaching has been described by the Russian physical chemist Mekler (1994), and the principle has been used to determine the fraction of acceptors clustering with donors in a cell biological realization of the technique (Szabó, Szöllősi, & Nagy, 2010).

CONSIDERATIONS FOR CHOOSING INSTRUMENTATION

In addition to choosing the approach for measuring FRET, another consideration is what kind of instrument to use. Spectrofluorimetry must be mentioned for historical reasons, as it is rarely used nowadays for cell biological FRET measurements. This approach reports the average fluorescence intensity of thousands of cells, which precludes discrimination between subpopulations. The contribution of cellular debris or dead cells to the measured signal cannot be considered either. Light scattering can be a significant issue, especially if a high density of cells or cells with a cell wall are measured (Hajdu et al., 2021). Furthermore, if fluorescence is due to labeling with a soluble ligand such as a fluorescent antibody, the presence of unbound fluorophores creates another source of error. Given these limitations, fluorometry is discouraged for cell biological FRET measurements.

Flow cytometry can provide quantitative measurements of thousands of individual cells in seconds, allowing convenient and rapid determination of the distribution of fluorescence intensities and energy transfer values in a population. Given the high-throughput nature of flow cytometry, this modality provides statistically robust data with cell-by-cell resolution. Flow cytometry is inherently incapable of achieving subcellular resolution or providing information about the time course of the response of a single cell. Furthermore, cells should be in suspension for flow cytometry, i.e., adherent cells should be detached mechanically or enzymatically. These treatments, however, can interfere with the cellular parameters to be investigated.

The widespread use of confocal microscopy revolutionized microscopic FRET investigations. Subcellular resolution, discrimination between cells based on their morphology, and time-course measurements of the same cell are obvious advantages of this measurement modality. In order to harness the full power of subcellular resolution, the area of interest should be identified in images, requiring image segmentation. Both the measurement and analysis of microscopic measurements are more labor-intensive than flow cytometry or fluorometry. The application of artificial neural networks and batch processing, such as with CellProfiler, can significantly speed up the evaluation.

Microscopy is limited by its relatively low throughput and subcellular resolution, while flow cytometry excels in speed but cannot provide insight into single cells. Imaging flow cytometry by Amnis and various automated microscopes can bridge the gap between flow and image cytometry (Basiji, 2016).

Microscopy offers another unique modality that deserves special consideration. The sensitivity of conventional fluorescence microscopy is sufficient for detecting single molecules, although emitters in greater proximity than the resolution limit (typically on the order of 200 nm) cannot be separated from each other. More distantly placed molecules can be observed as single, diffraction-limited spots. These single-molecule FRET methods offer unprecedented insight into molecular conformations, as FRET reports on distances on the nanometer scale, an achievement superior to even superresolution microscopy (Szabó et al., 2020). However, the single-molecular nature of such measurements requires special considerations. The orientation factor is much less likely to comply with or sufficiently approximate the dynamic averaging scheme, thus introducing errors in distance calculations. Therefore, it is important that fluorescent labels be connected to the molecules of interest via flexible linkers and the rotational hindrance imposed upon on the fluorescent labels by the linker must be estimated (Mazal & Haran, 2019; Sasmal, Pulido, Kasal, & Huang, 2016). The rest of the measurement and evaluation principles are identical to those of intensity-based FRET measurements: intensities are detected in the donor, FRET, and acceptor channels, followed by compensation for spectral spillover. However, if mobile single molecules are imaged, all three intensities must be measured on a timescale shorter than the diffusion time of single molecules through the detection volume of the objective. The laser lines exciting the donor and acceptor are therefore switched or interleaved very rapidly. Alternating laser excitation (ALEX) and pulsed interleaved excitation (PIE) both achieve this aim; they only differ in how quickly they change the excitation source (Hohlbein, Craggs, & Cordes, 2014; Muller, Zaychikov, Brauchle, & Lamb, 2005). In addition to determining single-molecule FRET efficiencies, i.e., single-molecule distances or conformations, the approach also reveals molecular stoichiometries, and the energy transfer efficiency and stoichiometry are plotted in two-parameter histograms (Hohlbein et al., 2014). Since the FRET efficiency can increase due to closer proximity of the acceptor to the donor or a higher number of acceptors surrounding the donor, differentiating between changes in stoichiometry and molecular distances is essential. Although resolution of conformational states is possible by constructing FRET histograms, hidden Markov models aid the differentiation between states that more closely resemble each other (Mazal & Haran, 2019; Talaga, 2007).

LIMITATIONS OF FRET STUDIES

Although application of FRET in biological research can be very useful, FRET approaches are associated with several limitations. As noted above, energy transfer depends on the dipole orientation of the fluorophores. Sometimes, FRET cannot be detected even in the presence of interaction due to the inappropriate orientation of the fluorophores, yielding false-negative results.

A low signal-to-noise ratio in microscopic FRET implementations could also lead to some obvious and some unexpected limitations. Low expression levels and low signals often prompt scientist to overexpress proteins or use overlabeled antibodies or high laser intensities. However, fluorophore conjugation has significant effects on the properties of the antibody and dye (Szabó et al., 2018). The fluorescence quantum yield of antibody-conjugated fluorophores decreases as a result of both dynamic and static quenching, with the latter being the dominant factor. Furthermore, the affinity of fluorescent antibodies decreases as a function of labeling, leading to a lower mean degree of labeling of the bound fraction than the antibody stock solution. These findings have important repercussions on experiments quantifying the fluorescence of antigen-bound antibodies, requiring consideration of the degree of labeling, such as determining parameter α in intensity-based or ratiometric FRET measurements (Szabó & Nagy, 2021). As a rule of thumb, determination of the degree of labeling and avoiding antibodies with a degree of labeling over 2 or 3 are suggested for quantitative fluorescence investigations.

Another issue of consideration when using antibody labeling is the size of the label and its cross-reactivity. Cross-reacting antibodies can bind to non-intended targets leading to errors in interpretation. Such problems can be alleviated by using monoclonal antibodies instead of polyclonals, and testing different monoclonal antibodies against the same target protein. The size of monoclonal antibodies is

not negligible compared to the labeled antigen or the distance range investigated in FRET measurements (Fig. 4 in (Jares-Erijman & Jovin, 2003)). FRET has been successfully implemented in samples primarily labeled with single chain antibodies, Fabs or antibodies, or after secondary labeling with fluorescent antibodies or streptavidin. There is no strict rule for how the size of the labeling complex affects FRET efficiencies, with some studies revealing such effects while others do not (König et al., 2006; Sebestyén et al., 2002). Therefore, we advise considering the potential effect of the size of the labeling complex on energy transfer efficiency.

Application of strong excitation intensity is also a way to increase the signal-to-noise ratio, but fluorophore saturation takes place at commonly applied excitation powers in confocal microscopy. If fluorophores are saturated, the emitted fluorescence is no longer linearly proportional to the excitation photon flux, which presents a major obstacle to standardization and can significantly distort FRET calculations. In particular, high excitation intensities leading to saturation of the donor lead to significant underestimations of FRET efficiency if the evaluation is performed without explicitly considering saturation phenomena (Szendi-Szatmári, Szabó, Szöllősi, & Nagy, 2019). Therefore, fluorophore saturation should be avoided or, if it is present, a formalism incorporating saturation phenomena must be used, such as the rFRET program (Nagy et al., 2016). These limitations, high degree of labeling and fluorophore saturation, are difficult to recognize without explicit attention paid to their discovery.

The achievable signal-to-noise ratio is also limited by cellular autofluorescence that is typically strong in the UV-blue range of the spectrum and usually exhibits a small Stokes shift. Consequently, autofluorescence can be curtailed by using dyes in the red spectral region or having large Stokes shifts. The measured fluorescence intensities should always be corrected for autofluorescence before performing the FRET calculations. If autofluorescence is relatively low, subtracting the mean autofluorescence from the measured intensities in each fluorescence channel is sufficient. Mean autofluorescence can be determined by measuring unlabeled or untransfected (mock-transfected) cells or by calculating the intensity in a cell-free area of an image in microscopy. If the magnitude of the signal is comparable to the autofluorescence, this correction approach can lead to significant problems. Cells exhibit heterogeneity with regard to their autofluorescence, so subtracting the average autofluorescence from a cell with low autofluorescence leads to overcompensation that can be spotted by a significant number of negative pixel values (microscopy) or negative cell intensities (flow cytometry). Like fluorescent dyes, autofluorescence is also characterized by a spectrum, and autofluorescence intensities measured in different fluorescence channels are correlated. By measuring autofluorescence in a channel that is not contaminated by the fluorescence of any of the fluorophores, autofluorescence can be subtracted on a pixel-by-pixel or cell-by-cell basis similar to compensation for spectral crosstalk. This approach provides superior results in measurements with a low signal-to-noise ratio (Sebestyén et al., 2002).

Another factor that can limit FRET detection is the donor-to-acceptor ratio if it lies outside the range between 10:1 and 1:10. This factor can be a serious limitation in FRET measurements of protein-protein interactions in which one of the partners is in excess. If the donor significantly outnumbers the acceptor, the majority of the donors may be acceptor-free. Even if the FRET efficiency of those donor-tagged proteins that can find an acceptor-labeled partner is high, the overwhelming majority of acceptor-free donors, which contribute a 0% FRET efficiency to the average, will result in a low FRET value. In this case, it may be worthwhile to consider swapping the tags on the proteins under investigation. However, acceptors highly outnumbering donors can also cause problems such as a higher probability of false positive results due to chance interactions. The effects of donor and acceptor abundance and their ratios on FRET efficiencies given random or clustered distribution have been studied in detail (Kenworthy & Edidin, 1998). Independent of the donor-acceptor ratio, it is always advisable to include positive and negative biological controls such that their expression levels are comparable to the expression of the proteins under investigation. Due to the fact that the expression level of donor- and acceptor-tagged targets is commonly a biological property that cannot or should not be changed, a host of possible protein-protein interactions do not lend themselves easily to FRET techniques. However, using fluorescent protein biosensors with only a single donor and acceptor ensures the stoichiometry is fixed at 1:1, avoiding the risk of error (Zadran et al., 2012).

The presence of spectral bleed-through (crosstalk) between spectrally overlapping fluorophores is also important to FRET calculations. Although FRET becomes more likely with increasing overlap between the donor emission and acceptor absorption spectra, the extent of bleed-through also becomes larger. Bleed-through typically refers to a fluorophore causing a signal in the fluorescence channel of another dye, e.g., the donor fluorophore causing a signal in the acceptor channel and vice versa or any fluorophore appearing in the FRET channel. To eliminate spectral crosstalk, corrections should be performed by measuring fluorescence intensities of donor- and acceptor-only labeled samples from which spectral crosstalk parameters can be determined (Shrestha, Jenei, Nagy, Vereb, & Szollosi, 2015).

Qdots are fluorophores containing a few hundred to a few thousand atoms of a semiconductor material forming an inorganic core surrounded by an organic outer layer of surfactant molecules. They are further functionalized, e.g., by antibodies or avidin, to allow them to be used as labels. Qdots have several advantages compared to organic dyes and fluorescent proteins, such as broader excitation spectra enabling excitation by a wide range of wavelengths, and they show narrower and more symmetric emission spectra. Moreover, Qdots are more stable against photobleaching due to their inorganic composition and have significantly longer fluorescence lifetimes. Depending on their size and chemical composition, they emit photons with different wavelengths (Alivisatos, Gu, & Larabell, 2005; Jovin, 2003). Although Qdots offer great photostability, they also have disadvantages. Their size is comparable to that of the labeled target, which affects lateral mobility (Váradi et al., 2019). In FRET studies, their size limits the available donor-acceptor distance, making them unsuitable for measuring distances. Furthermore, they are typically multivalent, which can lead to crosslinking. Qdots are not optimal FRET acceptors because the donor would also be excited due to the very wide absorption spectra (Barroso, 2011). To overcome this limitation luminescent lanthanide complexes with very long fluorescence lifetimes, or bioluminescent or chemiluminescent donors can be used along with a Qdot acceptor. Using a lanthanide-based donor and a Qdot acceptor, FRET can be detected within a longer distance, between 1 and 20 nm. Conversely, Qdots have been widely used as FRET donors (Barroso, 2011) in the development of diagnostic assays, target-specific in vitro and in vivo biosensors, light harvesting, and active nanodevices (Geissler & Hildebrandt, 2016).

APPLICATIONS

FRET has been applied in investigations of a large variety of objects and phenomena. In a series of studies, FRET was utilized to obtain otherwise difficult to observe structural information of various molecules *in situ* and *in vivo* (Feng, Poyton, & Ha, 2021; Gayrard & Borghi, 2016; Lerner et al., 2021; Pal, 2022; Terai, Imanishi, Li, & Matsuda, 2019; Voith von Voithenberg & Lamb, 2018). FRET has also been used to design high sensitivity sensors for various biological assays (Imani, Mohajeri, Rastegar, & Zarghami, 2021; Terai et al., 2019; Weihs, Anderson, Trowell, & Caron, 2021), and FRET has been extensively used in plant research (Duan, Li, Duan, Zhang, & Xing, 2022).

A detailed list of possible FRET applications is beyond the scope of this unit. Extensive reviews provide useful examples of FRET studies (Lerner et al., 2018; Lim, Petersen, Bunz, Simon, & Schindler, 2022; Shrestha et al., 2015; Szabó et al., 2020; Szalai, Zaza, & Stefani, 2021). We call attention to a few novel and interesting applications of new FRET methods such as new modalities of flow cytometry, developments in single molecule FRET (smFRET), FRET combined with high resolution and lifetime imaging microscopy (FLIM), and with molecular dynamics (MD) simulations.

Application of FRET analysis in flow cytometry provides a robust, high-throughput analysis of biological samples. Because a high number of cells can be analyzed within a short period of time, high statistical accuracy can be achieved in multiple samples (Lim et al., 2022). The popularity of flow cytometric FRET analysis in the last two decades is justified despite the fact that heterogeneity of FRET values within cells cannot be detected. The new developments in flow cytometry such as spectral flow cytometry and fluorescence lifetime flow cytometry open new possibilities for FRET analysis. It has been demonstrated that spectral flow cytometry provides more accurate FRET values than conventional flow cytometry (Henderson et al., 2021). While conventional flow cytometry uses the "3-cube method" for measuring intensity-based FRET values, spectral flow cytometry applies linear unmixing in the emission spectrum for multiple wavelength ranges for FRET calculations,

providing greater single cell precision even in the presence of other fluorophores and in real time (Henderson et al., 2021). Application of spectral flow cytometric FRET is a great step towards hyperdimensional flow cytometry (Bene & Damjanovich, 2022). New tandem fluorophores were created by utilizing the principle of FRET to broaden the application of spectral flow cytometry in the near-infrared region (Seong et al., 2022). Although fluorescence lifetime measurements in flow cytometry have been around for almost thirty years, only recently have they been applied for FRET measurements (Nichani, Li, Suzuki, & Houston, 2020). Flow cytometric frequency-domain measurements were utilized to measure the donor lifetime in the presence of acceptors. Houston et al. applied fluorogenic peptides to detect caspase activity using lifetime-based FRET measurements on a cell-by-cell basis and phasor representation for monitoring apoptosis (Nichani et al., 2020). Using special microfluidic flow cytometry, Nebdal and coworkers successfully applied time-domain lifetime measurements (which uses pulses instead of modulation) to establish a high-throughput FRET assay for monitoring the phosphorylation of epidermal growth factor receptor (Nedbal et al., 2015). Tong et al. monitored miRNA combination and degradation by FRET analysis in imaging flow cytometry (Tong et al., 2018).

Diffraction-limited FRET measurements provide information about the ensemble of donor and acceptor molecules, but the heterogeneity in FRET efficiency values between individual molecules is difficult or impossible to study. Furthermore, rare interactions with potentially important biological roles may not be detected (Lerner et al., 2018). The introduction of single molecule FRET (smFRET) has solved this problem since the FRET event is determined individually for single molecules. The smFRET technique can be performed by confocal microscopy, in which molecules freely diffuse into the observation volume, or in total internal reflection microscopy (TIRF), in which the molecules are immobilized. Since the first use of smFRET, which successfully detected conformational changes in macromolecules (Ha et al., 1996), the technique improved significantly. The author of this original paper has recently published a useful practical guide for quantitative smFRET (Roy, Hohng, & Ha, 2008). Slow conformational dynamics can be studied with immobilized molecules where the observation can range from 100 ms to 10 s (Kim, Lee, Hyeon, & Hong, 2015). Conformational changes in the 10 μs to 10 s range can be best studied using diffusion-based smFRET (Tomov et al., 2012). With the established and improved smFRET schemes, several problems have been studied, such as the structural dynamics of ion channels (Martinac, 2017), membrane proteins (Castell, Dijkman, Wiseman, & Goddard, 2018; Ward, Ye, Schuster, Wei, & Barrera, 2021; Yang, Xu, Wang, Chen, & Zhao, 2021), intrinsically disordered proteins (LeBlanc, Kulkarni, & Weninger, 2018; Metskas & Rhoades, 2020), DNA polymerases (Millar, 2022), and DNA nanostructures (Pal, 2022). The multicolor version of smFRET, in which more than one donor-acceptor pair is used, can provide even more information about protein-DNA interactions, chromatin remodeling and even protein translation (Feng et al., 2021).

FRET measurements have recently been combined with super-resolution fluorescence microscopy. The driving force of this combination was to create FRET-enhanced super-resolution imaging or super-resolved FRET imaging as it was nicely summarized by Szalai et al. (2021). Super-resolution microscopies are divided into two main categories: i) coordinate-stochastic methods such as Single Molecule Localization Microscopy (SMLM), Stochastic Optical Reconstruction Microscopy (STORM), and PhotoActivated Localization Microscopy (PALM); and ii) coordinate-targeted methods such as Stimulated Emission Depletion (STED) and Reversible Saturation Optical Fluorescence Transitions (RESOLFT) (Achimovich, Ai, & Gahlmann, 2019). Winckler et al. used a special coordinate-stochastic model, two-color universal Point Accumulation In the Nanoscale Topography (uPAINT) combined with FRET to detect EGFR dimerization in live cells, demonstrating that these dimerizations happen at the edge of the cells (Winckler et al., 2013). This method is slow because dyes should be turned on and off, and a large number of images should be applied to extract the necessary data. If we want to follow the kinetics of a process, intensity-based STED combined with FRET is a better approach. This approach is technically difficult; however, with appropriate controls Szalai et al. imaged biomolecular interactions in the membrane-associated cytoskeleton of a neuron with high optical resolution (Szalai et al., 2021). Although Structured Illumination Microscopy (SIM) improves optical resolution by only a factor of two, recent application of SIM with FRET made it possible to determine

FRET in live HeLa cells with reasonable optical resolution (Liu et al., 2022). Improving SIM could provide an attractive and simple alternative approach to enhance the resolution of FRET images.

FLIM FRET is a microscopy-based tool to monitor molecular associations under physiological conditions (Liput, Nguyen, Augustin, Lee, & Vogel, 2020). The two flavors of FLIM, frequency domain (Kremers, van Munster, Goedhart, & Gadella, 2008) and time domain (Becker, 2012), are available to determine the fluorescence lifetime of fluorophores. The frequency domain approach is less accurate but faster than the time domain approach and, because of the higher temporal resolution, it is preferred in live cell imaging. Although the time domain approach is more accurate, it requires sophisticated laser excitation systems (Larijani & Miles, 2022). FLIM FRET approaches have been successfully applied to monitoring DNA compaction (Levchenko, Pliss, Peng, Prasad, & Qu, 2021), screening signal transduction pathways (Ahmed, Schoberer, Cooke, & Botchway, 2021; Harkes et al., 2021; Kuo, Ho, Huang, & Chang, 2018), and for cancer diagnosis by detecting HER2-HER3 dimerization (Ouyang, Liu, Wang, Liu, & Wu, 2021; Weitsman et al., 2016). Combined measurements of acceptor bleaching and donor lifetime made it possible to investigate the dimeric and trimeric interacting states of molecules in a three-fluorophore system (Eckenstaler & Benndorf, 2021). Using different fluorescent proteins as donor and acceptor, Weber et al. monitored apoptosis with FLIM FRET in 3D cell cultures using light sheet microscopy while ensuring low light exposure (Weber et al., 2015). Two-photon excitation combined with FLIM FRET is a new imaging technique whose potential has been demonstrated by characterizing material transport between ovarian cancer cells through tunneling nanotubes (Wang et al., 2021) and by monitoring Rho GTPase activation in synapses with high spatial and temporal resolution (Ueda, Nagasawa, & Murakoshi, 2022).

Classical FRET analysis and MD simulations have been combined to provide hints about possible orientations and arrangements of membrane-bound HER2 molecules. The data analysis proved that HER2 molecules form homodimers and the modeling revealed a structure with three potential interacting regions (Bagossi, Horváth, Vereb, Szöllősi, & Tőzsér, 2005). New developments in smFRET helped combine FRET and MD simulations even more effectively (Barth et al., 2022). MD simulations performed in the same time range as smFRET were consistent with the smFRET data and facilitated the interpretation of fluorophore distances and orientations (Girodat, Pati, Terry, Blanchard, & Sanbonmatsu, 2020). Combining smFRET with MD simulation revealed the dynamics of strand slipping in DNA hairpins (Xu, Pan, Roland, Sagui, & Weninger, 2020) and the dependence of the conformational dimensionality of single-stranded poly(T) DNA on the NaCl concentration (Kim & Lee, 2021). Wruck and coworkers used an optical tweezer with smFRET and MD simulations to show that the ribosome exit channel accelerates folding and stabilizes the folding states of exiting proteins (Wruck et al., 2021).

Since Förster first established FRET analysis in 1946, its utilization has increased tremendously in biological research. Technical improvements in flow cytometry (spectral and fluorescence lifetime resolved flow cytometry), microscopy (single molecular detection, super-resolution, and time-resolved microscopy), and the development of new fluorescent probes with better photophysical properties open up new avenues for employing modern FRET methods inventively and effectively in deciphering the mechanisms of important biological processes.

CONCLUDING REMARKS

This unit presents a solid theoretical basis for how to design and evaluate FRET experiments critically taking all the pros and cons into consideration. While the physical and technical details may sometimes seem unnecessary, the physical and predictable nature of the process is a clear advantage since the limitations of the method can be defined on a solid basis. Consequently, FRET approaches are viable alternatives for measuring oligomerization and molecular structure even in the era of superresolution techniques.

ACKNOWLEDGMENTS

This work was supported by research grants K138075, ANN133421, and GINOP-2.2.1–15-2017–00044 from the National Research, Development and Innovation Office, Hungary.

AUTHOR CONTRIBUTIONS

Agnes Szabo: Original draft, review, and editing. **János Szöllősi:** Conceptualization; Original draft, review, and editing. **Peter Nagy:** Conceptualization; Funding acquisition; Original draft, review, and editing.

CONFLICT OF INTEREST

The authors declare no conflict of interest.

DATA AVAILABILITY STATEMENT

Data sharing not applicable – no new data generated, or the article describes entirely theoretical research.

Literature Cited

Achimovich, A. M., Ai, H., & Gahlmann, A. (2019). Enabling technologies in super-resolution fluorescence microscopy: Reporters, labeling, and methods of measurement. *Current Opinion in Structural Biology*, *58*, 224–232. doi: 10.1016/j.sbi.2019.05.001

Ahmed, A., Schoberer, J., Cooke, E., & Botchway, S. W. (2021). Multicolor FRET-FLIM microscopy to analyze multiprotein interactions in live cells. *Methods in Molecular Biology*, *2247*, 287–301. doi: 10.1007/978-1-0716-1126-5_16

Alivisatos, A. P., Gu, W., & Larabell, C. (2005). Quantum dots as cellular probes. *Annual Review of Biomedical Engineering*, *7*, 55–76. doi: 10.1146/annurev.bioeng.7.060804.100432

Bagossi, P., Horváth, G., Vereb, G., Szöllősi, J., & Tőzsér, J. (2005). Molecular modeling of nearly full-length ERBB2 receptor. *Biophysical Journal*, *88*(2), 1354–1363. doi: 10.1529/biophysj.104.046003

Barroso, M. M. (2011). Quantum dots in cell biology. *Journal of Histochemistry & Cytochemistry*, *59*(3), 237–251. doi: 10.1369/0022155411398487

Barth, A., Opanasyuk, O., Peulen, T. O., Felekyan, S., Kalinin, S., Sanabria, H., & Seidel, C. A. M. (2022). Unraveling multi-state molecular dynamics in single-molecule FRET experiments. I. Theory of FRET-lines. *The Journal of Chemical Physics*, *156*(14), 141501. doi: 10.1063/5.0089134

Basiji, D. A. (2016). Principles of amnis imaging flow cytometry. *Methods in Molecular Biology*, *1389*, 13–21. doi: 10.1007/978-1-4939-3302-0_2

Bastiaens, P. I., Majoul, I. V., Verveer, P. J., Soling, H. D., & Jovin, T. M. (1996). Imaging the intracellular trafficking and state of the ab5 quaternary structure of cholera toxin. *EMBO Journal*, *15*(16), 4246–4253.

Becker, W. (2012). Fluorescence lifetime imaging–techniques and applications. *Journal of Microscopy*, *247*(2), 119–136. doi: 10.1111/j.1365-2818.2012.03618.x

Bene, L., & Damjanovich, L. (2022). Spectral flow cytometric FRET: Towards a hyper dimensional flow cytometry. *Cytometry A*, *101*(6), 468–473. doi: 10.1002/cyto.a.24561

Bene, L., Fulwyler, M. J., & Damjanovich, S. (2000). Detection of receptor clustering by flow cytometric fluorescence anisotropy measurements. *Cytometry*, *40*(4), 292–306. doi: 10.1002/1097-0320(20000801)40:4<292::AID-CYTO5>3.0.CO;2-%23.

Bene, L., Szöllősi, J., Szentesi, G., Damjanovich, L., Gáspár, R., Jr., Waldmann, T. A., & Damjanovich, S. (2005). Detection of receptor trimers on the cell surface by flow cytometric fluorescence energy homotransfer measurements. *Biochimica et Biophysica Acta*, *1744*(2), 176–198. doi: 10.1016/j.bbamcr.2005.02.002

Beutler, M., Makrogianneli, K., Vermeij, R. J., Keppler, M., Ng, T., Jovin, T. M., & Heintzmann, R. (2008). SatFRET: Estimation of Förster resonance energy transfer by acceptor saturation. *European Biophysics Journal*, *38*(1), 69–82. doi: 10.1007/s00249-008-0361-5

Castell, O. K., Dijkman, P. M., Wiseman, D. N., & Goddard, A. D. (2018). Single molecule fluorescence for membrane proteins. *Methods*, *147*, 221–228. doi: 10.1016/j.ymeth.2018.05.024

Chen, Y., Mauldin, J. P., Day, R. N., & Periasamy, A. (2007). Characterization of spectral FRET imaging microscopy for monitoring nuclear protein interactions. *Journal of Microscopy*, *228*(Pt2), 139–152. doi: 10.1111/j.1365-2818.2007.01838.x

Clegg, R. M. (2009). Förster resonance energy transfer—FRET what is it, why do it, and how it's done. In T. W. J. Gadella (Ed.), *Laboratory techniques in biochemistry and molecular biology* Vol. *33* (pp. 1–57). Amsterdam: Elsevier. doi: 10.1016/S0075-7535(08)00001-6

Dale, R. E., & Eisinger, J. (1974). Intramolecular distances determined by energy transfer. Dependence on orientational freedom of donor and acceptor. *Biopolymers*, *13*(8), 1573–1605. doi: 10.1002/bip.1974.360130807

Duan, Z., Li, K., Duan, W., Zhang, J., & Xing, J. (2022). Probing membrane protein interactions and signaling molecule homeostasis in plants by Förster resonance energy transfer analysis. *Journal of Experimental Botany*, *73*(1), 68–77. doi: 10.1093/jxb/erab445

Eckenstaler, R., & Benndorf, R. A. (2021). A combined acceptor photobleaching and donor fluorescence lifetime imaging microscopy approach to analyze multi-protein interactions in living cells. *Frontiers in Molecular Biosciences*, *8*, 635548. doi: 10.3389/fmolb.2021.635548

Evers, T. H., van Dongen, E. M., Faesen, A. C., Meijer, E. W., & Merkx, M. (2006). Quantitative understanding of the energy transfer between fluorescent proteins connected via flexible peptide linkers. *Biochemistry*, *45*(44), 13183–13192. doi: 10.1021/bi061288t

Feng, X. A., Poyton, M. F., & Ha, T. (2021). Multicolor single-molecule FRET for DNA and RNA processes. *Current Opinion in Structural Biology*, *70*, 26–33. doi: 10.1016/j.sbi.2021.03.005

Förster, T. (1946). Energiewanderung und fluoreszenz. *Naturwissenschaften*, *33*(6), 166–175. doi: 10.1007/BF00585226

Gayrard, C., & Borghi, N. (2016). FRET-based molecular tension microscopy. *Methods*, *94*, 33–42. doi: 10.1016/j.ymeth.2015.07.010

Geissler, D., & Hildebrandt, N. (2016). Recent developments in forster resonance energy

transfer (FRET) diagnostics using quantum dots. *Analytical and Bioanalytical Chemistry*, *408*(17), 4475–4483. doi: 10.1007/s00216-016-9434-y

Girodat, D., Pati, A. K., Terry, D. S., Blanchard, S. C., & Sanbonmatsu, K. Y. (2020). Quantitative comparison between sub-millisecond time resolution single-molecule fret measurements and 10-second molecular simulations of a biosensor protein. *PLOS Computational Biology*, *16*(11), e1008293. doi: 10.1371/journal.pcbi.1008293

Griffiths, D. J. (2013). The electric field of a dipole. In *Introduction to electrodynamics* (pp. 158–159). Boston: Pearson.

Ha, T., Enderle, T., Ogletree, D. F., Chemla, D. S., Selvin, P. R., & Weiss, S. (1996). Probing the interaction between two single molecules: Fluorescence resonance energy transfer between a single donor and a single acceptor. *Proceedings of the National Academy of Sciences USA*, *93*(13), 6264–6268. doi: 10.1073/pnas.93.13.6264

Hajdu, T., Szabó, K., Jakab, Á., Pócsi, I., Dombrádi, V., & Nagy, P. (2021). Biophysical experiments reveal a protective role of protein phosphatase Z1 against oxidative damage of the cell membrane in *Candida albicans*. *Free Radical Biology and Medicine*, *176*, 222–227. doi: 10.1016/j.freeradbiomed.2021.09.020

Harkes, R., Kukk, O., Mukherjee, S., Klarenbeek, J., van den Broek, B., & Jalink, K. (2021). Dynamic FRET-FLIM based screening of signal transduction pathways. *Science Report*, *11*(1), 20711. doi: 10.1038/s41598-021-00098-9

Henderson, J., Havranek, O., Ma, M. C. J., Herman, V., Kupcova, K., Chrbolkova, T., … Davis, R. E. (2021). Detecting förster resonance energy transfer in living cells by conventional and spectral flow cytometry. *Cytometry A*, *101*(10), 818–834. doi: 10.1002/cyto.a.24472 Online ahead of print

Hohlbein, J., Craggs, T. D., & Cordes, T. (2014). Alternating-laser excitation: Single-molecule FRET and beyond. *Chemical Society Reviews*, *43*(4), 1156–1171. doi: 10.1039/c3cs60233h

Imani, M., Mohajeri, N., Rastegar, M., & Zarghami, N. (2021). Recent advances in FRET-based biosensors for biomedical applications. *Analytical Biochemistry*, *630*, 114323. doi: 10.1016/j.ab.2021.114323

Jares-Erijman, E. A., & Jovin, T. M. (2003). FRET imaging. *Nature Biotechnology*, *21*(11), 1387–1395. doi: 10.1038/nbt896nbt896

Jovin, T. M. (2003). Quantum dots finally come of age. *Nature Biotechnology*, *21*(1), 32–33. doi: 10.1038/nbt0103-32

Kenworthy, A. K., & Edidin, M. (1998). Distribution of a glycosylphosphatidylinositol-anchored protein at the apical surface of MDCK cells examined at a resolution of <100 Å using imaging fluorescence resonance energy transfer. *Journal of Cell Biology*, *142*(1), 69–84.

Kim, S. E., Lee, I. B., Hyeon, C., & Hong, S. C. (2015). Deciphering kinetic information from single-molecule FRET data that show slow transitions. *Journal of Physical Chemistry B*, *119*(23), 6974–6978. doi: 10.1021/acs.jpcb.5b03991

Kim, S. H., & Lee, T. H. (2021). Conformational dynamics of poly(T) single-stranded DNA at the single-molecule level. *Journal of Physical Chemistry Letters*, *12*(19), 4576–4584. doi: 10.1021/acs.jpclett.1c00962

Knox, R. S., & van Amerongen, H. (2002). Refractive index dependence of the Förster resonance excitation transfer rate. *The Journal of Physical Chemistry B*, *106*(20), 5289–5293. doi: 10.1021/jp013927+

König, P., Krasteva, G., Tag, C., König, I. R., Arens, C., & Kummer, W. (2006). FRET-CLSM and double-labeling indirect immunofluorescence to detect close association of proteins in tissue sections. *Laboratory Investigation*, *86*(8), 853–864. doi: 10.1038/labinvest.3700443

Kremers, G. J., van Munster, E. B., Goedhart, J., & Gadella, T. W., Jr. (2008). Quantitative lifetime unmixing of multiexponentially decaying fluorophores using single-frequency fluorescence lifetime imaging microscopy. *Biophysical Journal*, *95*(1), 378–389. doi: 10.1529/biophysj.107.125229

Kuo, H. L., Ho, P. C., Huang, S. S., & Chang, N. S. (2018). Chasing the signaling run by tri-molecular time-lapse fret microscopy. *Cell Death Discovery*, *4*, 45. doi: 10.1038/s41420-018-0047-4

Lakowicz, J. R. (2006a). Energy transfer. In Lakowicz, J. R. (Ed.), *Principles of Fluorescence Spectroscopy* (pp. 443–475). New York: Springer. doi: 10.1007/978-0-387-46312-4_13

Lakowicz, J. R. (2006b). Energy transfer to multiple acceptors in one, two, or three dimensions. In Lakowicz, J. R. (Ed.), *Principles of fluorescence spectroscopy* (pp. 507–528). New York: Springer. doi: 10.1007/978-0-387-46312-4_15

Lakowicz, J. R. (2006c). Fluorescence anisotropy. In Lakowicz, J. R. (Ed.), *Principles of fluorescence spectroscopy* (pp. 353–382). New York: Springer. doi: 10.1007/978-0-387-46312-4_10

Larijani, B., & Miles, J. (2022). Quantification of protein-protein interactions and activation dynamics: A new path to predictive biomarkers. *Biophysical Chemistry*, *283*, 106768. doi: 10.1016/j.bpc.2022.106768

Leavesley, S. J., Britain, A. L., Cichon, L. K., Nikolaev, V. O., & Rich, T. C. (2013). Assessing FRET using spectral techniques. *Cytometry A*, *83*(10), 898–912. doi: 10.1002/cyto.a.22340

LeBlanc, S. J., Kulkarni, P., & Weninger, K. R. (2018). Single molecule FRET: A powerful tool to study intrinsically disordered proteins. *Biomolecules*, *8*(4), 140. doi: 10.3390/biom8040140

Lerner, E., Barth, A., Hendrix, J., Ambrose, B., Birkedal, V., Blanchard, S. C., & Weiss, S. (2021). FRET-based dynamic structural biology: Challenges, perspectives and an appeal for open-science practices.

Elife, *10*, e60416. doi: 10.7554/eLife.60416

Lerner, E., Cordes, T., Ingargiola, A., Alhadid, Y., Chung, S., Michalet, X., & Weiss, S. (2018). Toward dynamic structural biology: Two decades of single-molecule Förster resonance energy transfer. *Science*, *359*(6373), eaan1133. doi: 10.1126/science.aan1133

Levchenko, S. M., Pliss, A., Peng, X., Prasad, P. N., & Qu, J. (2021). Fluorescence lifetime imaging for studying DNA compaction and gene activities. *Light: Science & Applications*, *10*(1), 224. doi: 10.1038/s41377-021-00664-w

Lidke, D. S., Nagy, P., Barisas, B. G., Heintzmann, R., Post, J. N., Lidke, K. A., … Jovin, T. M. (2003). Imaging molecular interactions in cells by dynamic and static fluorescence anisotropy (rFLIM and emFRET). *Biochemical Society Transactions*, *31*(Pt 5), 1020–1027. doi: 10.1042/bst0311020

Lim, J., Petersen, M., Bunz, M., Simon, C., & Schindler, M. (2022). Flow cytometry-based FRET: Basics, novel developments and future perspectives. *Cellular and Molecular Life Sciences*, *79*(4), 217. doi: 10.1007/s00018-022-04232-2

Liput, D. J., Nguyen, T. A., Augustin, S. M., Lee, J. O., & Vogel, S. S. (2020). A guide to fluorescence lifetime microscopy and Förster's resonance energy transfer in neuroscience. *Current Protocols in Neuroscience*, *94*(1), e108. doi: 10.1002/cpns.108

Liu, Z., Luo, Z., Chen, H., Yin, A., Sun, H., Zhuang, Z., & Chen, T. (2022). Optical section structured illumination-based Förster resonance energy transfer imaging. *Cytometry A*, *101*(3), 264–272. doi: 10.1002/cyto.a.24500

Marcus, R. A. (1993). Electron transfer reactions in chemistry. Theory and experiment. *Reviews of Modern Physics*, *65*(3), 599–610. doi: 10.1103/RevModPhys.65.599

Martinac, B. (2017). Single-molecule FRET studies of ion channels. *Progress in Biophysics and Molecular Biology*, *130*(Pt B), 192–197. doi: 10.1016/j.pbiomolbio.2017.06.014

Matkó, J., Jenei, A., Mátyus, L., Ameloot, M., & Damjanovich, S. (1993). Mapping of cell surface protein-patterns by combined fluorescence anisotropy and energy transfer measurements. *Journal of Photochemistry and Photobiology B*, *19*(1), 69–73.

Mazal, H., & Haran, G. (2019). Single-molecule fret methods to study the dynamics of proteins at work. *Current Opinion in Biomedical Engineering*, *12*, 8–17. doi: 10.1016/j.cobme.2019.08.007

Mekler, V. M. (1994). A photochemical technique to enhance sensitivity of detection of fluorescence resonance energy transfer. *Photochemistry and Photobiology*, *59*, 615–620. doi: 10.1111/j.1751-1097.1994.tb08227.x

Metskas, L. A., & Rhoades, E. (2020). Single-molecule FRET of intrinsically disordered proteins. *Annual Review of Physical Chemistry*, *71*, 391–414. doi: 10.1146/annurev-physchem-012420-104917

Millar, D. P. (2022). Conformational dynamics of DNA polymerases revealed at the single-molecule level. *Frontiers in Molecular Biosciences*, *9*, 826593. doi: 10.3389/fmolb.2022.826593

Muller, B. K., Zaychikov, E., Brauchle, C., & Lamb, D. C. (2005). Pulsed interleaved excitation. *Biophysical Journal*, *89*(5), 3508–3522. doi: 10.1529/biophysj.105.064766

Nagy, P., Szabó, Á., Váradi, T., Kovács, T., Batta, G., & Szöllősi, J. (2016). RFRET: A comprehensive, matlab-based program for analyzing intensity-based ratiometric microscopic FRET experiments. *Cytometry A*, *89*(4), 376–384. doi: 10.1002/cyto.a.22828

Nagy, P., Vereb, G., Damjanovich, S., Mátyus, L., & Szöllősi, J. (2006). Measuring FRET in flow cytometry and microscopy. In J. P. Robinson (Ed.), *Current protocols in cytometry* (pp. 12.18.11–12.18.13). New York: John Wiley & Sons.

Nedbal, J., Visitkul, V., Ortiz-Zapater, E., Weitsman, G., Chana, P., Matthews, D. R., … Ameer-Beg, S. M. (2015). Time-domain microfluidic fluorescence lifetime flow cytometry for high-throughput Förster resonance energy transfer screening. *Cytometry A*, *87*(2), 104–118. doi: 10.1002/cyto.a.22616

Nichani, K., Li, J., Suzuki, M., & Houston, J. P. (2020). Evaluation of caspase-3 activity during apoptosis with fluorescence lifetime-based cytometry measurements and phasor analyses. *Cytometry A*, *97*(12), 1265–1275. doi: 10.1002/cyto.a.24207

Ouyang, Y., Liu, Y., Wang, Z. M., Liu, Z., & Wu, M. (2021). FLIM as a promising tool for cancer diagnosis and treatment monitoring. *Nano-Micro Letters*, *13*(1), 133. doi: 10.1007/s40820-021-00653-z

Pal, N. (2022). Single-molecule FRET: A tool to characterize DNA nanostructures. *Frontiers in Molecular Biosciences*, *9*, 835617. doi: 10.3389/fmolb.2022.835617

Perrin, F. (1929). La fluorescence des solutions. *Annals of Physics (Paris)*, *12*, 169–275.

Perrin, F. (1932). Théorie quantique des transferts d'activation entre molécules de méme espéce. Cas des solutions fluorescentes. *Annals of Physics (Paris)*, *17*, 283–314.

Roberti, M. J., Giordano, L., Jovin, T. M., & Jares-Erijman, E. A. (2011). FRET imaging by k(t)/k(f). *Chemphyschem*, *12*(3), 563–566. doi: 10.1002/cphc.201000925

Roy, R., Hohng, S., & Ha, T. (2008). A practical guide to single-molecule FRET. *Nature Methods*, *5*(6), 507–516. doi: 10.1038/nmeth.1208

Runnels, L. W., & Scarlata, S. F. (1995). Theory and application of fluorescence homotransfer to melittin oligomerization. *Biophysical Journal*, *69*(4), 1569–1583.

Sasmal, D. K., Pulido, L. E., Kasal, S., & Huang, J. (2016). Single-molecule fluorescence

resonance energy transfer in molecular biology. *Nanoscale*, *8*(48), 19928–19944. doi: 10.1039/c6nr06794h

Sebestyén, Z., Nagy, P., Horváth, G., Vámosi, G., Debets, R., Gratama, J. W., & Szöllősi, J. (2002). Long wavelength fluorophores and cell-by-cell correction for autofluorescence significantly improves the accuracy of flow cytometric energy transfer measurements on a dual-laser benchtop flow cytometer. *Cytometry*, *48*(3), 124–135. doi: 10.1002/cyto.10121

Seong, Y., Nguyen, D. X., Wu, Y., Thakur, A., Harding, F., & Nguyen, T. A. (2022). Novel PE and APC tandems: Additional near-infrared fluorochromes for use in spectral flow cytometry. *Cytometry A*, *100*(10), 835–845. doi: 10.1002/cyto.a.24537 Online ahead of print

Shrestha, D., Jenei, A., Nagy, P., Vereb, G., & Szollosi, J. (2015). Understanding FRET as a research tool for cellular studies. *International Journal of Molecular Sciences*, *16*(4), 6718–6756. doi: 10.3390/ijms16046718

Song, L., Jares-Erijman, E. A., & Jovin, T. M. (2002). A photochromic acceptor as a reversible light-driven switch in fluorescence resonance energy transfer (FRET). *Journal of Photochemistry and Photobiology A: Chemistry*, *150*(1–3), 177–185. doi: 10.1016/S1010-6030(02)00129-6

Stryer, L. (1978). Fluorescence energy transfer as a spectroscopic ruler. *Annual Review of Biochemistry*, *47*, 819–846. doi: 10.1146/annurev.bi.47.070178.004131

Stryer, L., & Haugland, R. P. (1967). Energy transfer: A spectroscopic ruler. *Proceedings of the National Academy of Sciences USA*, *58*(2), 719–726. doi: 10.1073/pnas.58.2.719

Szabó, Á., Horváth, G., Szöllősi, J., & Nagy, P. (2008). Quantitative characterization of the large-scale association of ERBB1 and ERBB2 by flow cytometric homo-FRET measurements. *Biophysical Journal*, *95*(4), 2086–2096. doi: biophysj.108.133371[pii]10.1529/biophysj.108.133371.

Szabó, Á., & Nagy, P. (2021). I am the alpha and the …Gamma, and the g. Calibration of intensity-based FRET measurements. *Cytometry A*, *99*(4), 369–371. doi: 10.1002/cyto.a.24206

Szabó, A., Szendi-Szatmári, T., Szöllősi, J., & Nagy, P. (2020). Quo vadis FRET? Förster's method in the era of superresolution. *Methods and Applications in Fluorescence*, *8*(3), 032003. doi: 10.1088/2050-6120/ab9b72

Szabó, Á., Szendi-Szatmári, T., Ujlaky-Nagy, L., Rádi, I., Vereb, G., Szöllősi, J., & Nagy, P. (2018). The effect of fluorophore conjugation on antibody affinity and the photophysical properties of dyes. *Biophysical Journal*, *114*(3), 688–700. doi: 10.1016/j.bpj.2017.12.011

Szabó, A., Szöllősi, J., & Nagy, P. (2010). Coclustering of ERBB1 and ERBB2 revealed by FRET-sensitized acceptor bleaching. *Biophysical Journal*, *99*(1), 105–114. doi: S0006-3495(10)00428-5[pii]10.1016/j.bpj.2010.03.061.

Szalai, A. M., Siarry, B., Lukin, J., Giusti, S., Unsain, N., Caceres, A., … Stefani, F. D. (2021). Super-resolution imaging of energy transfer by intensity-based STED-FRET. *Nano Letters*, *21*(5), 2296–2303. doi: 10.1021/acs.nanolett.1c00158

Szalai, A. M., Zaza, C., & Stefani, F. D. (2021). Super-resolution FRET measurements. *Nanoscale*, *13*(44), 18421–18433. doi: 10.1039/d1nr05769c

Szendi-Szatmári, T., Szabó, Á., Szöllősi, J., & Nagy, P. (2019). Reducing the detrimental effects of saturation phenomena in FRET microscopy. *Analytical Chemistry*, *91*(9), 6378–6382. doi: 10.1021/acs.analchem.9b01504

Talaga, D. S. (2007). Markov processes in single molecule fluorescence. *Current Opinion in Colloid & Interface Science*, *12*(6), 285–296. doi: 10.1016/j.cocis.2007.08.014

Terai, K., Imanishi, A., Li, C., & Matsuda, M. (2019). Two decades of genetically encoded biosensors based on Förster resonance energy transfer. *Cell Structure and Function*, *44*(2), 153–169. doi: 10.1247/csf.18035

Thaler, C., Koushik, S. V., Blank, P. S., & Vogel, S. S. (2005). Quantitative multiphoton spectral imaging and its use for measuring resonance energy transfer. *Biophysical Journal*, *89*(4), 2736–2749. doi: 10.1529/biophysj.105.061853

Tomov, T. E., Tsukanov, R., Masoud, R., Liber, M., Plavner, N., & Nir, E. (2012). Disentangling subpopulations in single-molecule FRET and ALEX experiments with photon distribution analysis. *Biophysical Journal*, *102*(5), 1163–1173. doi: 10.1016/j.bpj.2011.11.4025

Tong, Q., Zhu, Y., Zhang, D., Cai, Q., Qu, W., Cooper, C. D. O., … McHugh, P. C. (2018). MicroRNA quantitation during dendritic cell endocytosis using imaging flow cytometry: Key factors and requirements. *Cellular Physiology and Biochemistry*, *51*(2), 793–811. doi: 10.1159/000495333

Ueda, H. H., Nagasawa, Y., & Murakoshi, H. (2022). Imaging intracellular protein interactions/activity in neurons using 2-photon fluorescence lifetime imaging microscopy. *Neuroscience Research*, *179*, 31–38. doi: 10.1016/j.neures.2021.10.004

van der Meer, B. W. (2002). Kappa-squared: From nuisance to new sense. *Journal of Biotechnology*, *82*(3), 181–196.

van der Meer, B. W. (2013). Förster theory. In I. Medintz & N. Hildebrandt (Eds.) *FRET – Förster resonance energy transfer* (pp. 23–62). Hoboken, NJ: Wiley.

van der Meer, B. W. (2020). Kappaphobia is the elephant in the FRET room. *Methods and Applications in Fluorescence*, *8*(3), 030401. doi: 10.1088/2050-6120/ab8f87

van der Meer, B. W., van der Meer, D. M., & Vogel, S. S. (2013). Optimizing the orientation factor kappa-squared for more accurate FRET measurements. In I. Medintz & N. Hildebrandt (Eds.) *FRET – Förster resonance energy transfer* (pp. 63–104). Hoboken, NJ: Wiley.

Váradi, T., Schneider, M., Sevcsik, E., Kiesenhofer, D., Baumgart, F., Batta, G., … Nagy, P. (2019). Homo- and heteroassociations drive activation of ERBB3. *Biophys J*, *117*(10), 1935–1947. doi: 10.1016/j.bpj.2019.10.001

Voith von Voithenberg, L., & Lamb, D. C. (2018). Single pair Förster resonance energy transfer: A versatile tool to investigate protein conformational dynamics. *Bioessays*, *40*(3). doi: 10.1002/bies.201700078

Wang, S., Li, Y., Zhao, Y., Lin, F., Qu, J., & Liu, L. (2021). Investigating tunneling nanotubes in ovarian cancer based on two-photon excitation FLIM-FRET. *Biomedical Optics Express*, *12*(4), 1962–1973. doi: 10.1364/BOE.418778

Ward, A. E., Ye, Y., Schuster, J. A., Wei, S., & Barrera, F. N. (2021). Single-molecule fluorescence vistas of how lipids regulate membrane proteins. *Biochemical Society Transactions*, *49*(4), 1685–1694. doi: 10.1042/BST20201074

Weber, P., Schickinger, S., Wagner, M., Angres, B., Bruns, T., & Schneckenburger, H. (2015). Monitoring of apoptosis in 3D cell cultures by FRET and light sheet fluorescence microscopy. *International Journal of Molecular Sciences*, *16*(3), 5375–5385. doi: 10.3390/ijms16035375

Weihs, F., Anderson, A., Trowell, S., & Caron, K. (2021). Resonance energy transfer-based biosensors for point-of-need diagnosis-progress and perspectives. *Sensors (Basel)*, *21*(2), 660. doi: 10.3390/s21020660

Weitsman, G., Barber, P. R., Nguyen, L. K., Lawler, K., Patel, G., Woodman, N., … Ng, T. (2016). Her2-her3 dimer quantification by FLIM-FRET predicts breast cancer metastatic relapse independently of HER2 IHC status. *Oncotarget*, *7*(32), 51012–51026. doi: 10.18632/oncotarget.9963

Winckler, P., Lartigue, L., Giannone, G., de Giorgi, F., Ichas, F., Sibarita, J. B., … Cognet, L. (2013). Identification and super-resolution imaging of ligand-activated receptor dimers in live cells. *Science Report*, *3*, 2387. doi: 10.1038/srep02387

Wlodarczyk, J., Woehler, A., Kobe, F., Ponimaskin, E., Zeug, A., & Neher, E. (2007). Analysis of FRET-signals in the presence of free donors and acceptors. *Biophysical Journal*, *94*(3), 986–1000. doi: biophysj.107.111773 [pii]10.1529/biophysj.107.111773[doi].

Wruck, F., Tian, P., Kudva, R., Best, R. B., von Heijne, G., Tans, S. J., & Katranidis, A. (2021). The ribosome modulates folding inside the ribosomal exit tunnel. *Communications Biology*, *4*(1), 523. doi: 10.1038/s42003-021-02055-8

Xu, P., Pan, F., Roland, C., Sagui, C., & Weninger, K. (2020). Dynamics of strand slippage in DNA hairpins formed by CAG repeats: Roles of sequence parity and trinucleotide interrupts. *Nucleic Acids Research*, *48*(5), 2232–2245. doi: 10.1093/nar/gkaa036

Yang, Z., Xu, H., Wang, J., Chen, W., & Zhao, M. (2021). Single-molecule fluorescence techniques for membrane protein dynamics analysis. *Applied Spectroscopy*, *75*(5), 491–505. doi: 10.1177/00037028211009973

Yeow, E. K., & Clayton, A. H. (2007). Enumeration of oligomerization states of membrane proteins in living cells by homo-FRET spectroscopy and microscopy: Theory and application. *Biophysical Journal*, *92*(9), 3098–3104. doi: 92/9/3098 [pii]10.1529/biophysj.106.099424.

Zadran, S., Standley, S., Wong, K., Otiniano, E., Amighi, A., & Baudry, M. (2012). Fluorescence resonance energy transfer (FRET)-based biosensors: Visualizing cellular dynamics and bioenergetics. *Applied Microbiology and Biotechnology*, *96*(4), 895–902. doi: 10.1007/s00253-012-4449-6

Zeug, A., Woehler, A., Neher, E., & Ponimaskin, E. G. (2012). Quantitative intensity-based FRET approaches—a comparative snapshot. *Biophysical Journal*, *103*(9), 1821–1827. doi: 10.1016/j.bpj.2012.09.031

Corrections

In this publication, the following corrections have been made:

In Table 1, the words "Donor excitation wavelength" are inserted into the blank space in row 3, and words "Acceptor emission wavelengths" are inserted into the blank space in row 4.

The current version online now includes these corrections and may be considered the authoritative version of record.